



Characterization of Potential Refractory Utilization of Blended Sabon-Gari and Bandawa Clays Collected from Deposits in Jalingo and Karim-Lamido Local Government Areas, Taraba State, Nigeria

^{1,2*}IDU, HK; ³SILAS, E

^{1*}Department of Industrial and Medical Physics, David Umahi Federal University of Health Sciences, Iburu, Ebonyi State, Nigeria

²International Institute of Nuclear Medicine & Allied Health Research, DUFUHS, Uburu, Ebonyi State, Nigeria

³Taraba State Community and Social Development Agency (CSDA), Jalingo, Taraba State, Nigeria

*Corresponding author, Email address: iduhyacinthkevin@gmail.com

*ORCID: <https://orcid.org/0000-0002-2555-8946>

*Tel: +2347087005115

Co-Author Email: ezesila@gmail.com

ABSTRACT: The objective of this paper was to evaluate the Characterization of Potential Refractory Utilization of Blended Sabon-Gari and Bandawa Clays collected from Deposits in the Jalingo and Karim-Lamido Local Government Areas, Taraba State, Nigeria. The results showed that the 20:80 mixture had the best performance index of all properties. The 20:80 mixture was then subjected to further XRD, FTIR and thermal conductivity analysis. The XRD pattern of the 20:80 mixture showed the predominant presence of montmorillonite, orthoclase, muscovite, albite and quartz. The FTIR spectrum showed bond stretching and bending vibrations associated with the hydroxyl group (OH), Si-O and Si-O-Si molecules, consistent with clay minerals. A nearly constant peak/intensity profile in the FTIR spectrum of the fired 20:80 mixture was observed in the wave number range of 1300 cm⁻¹ to 4000 cm⁻¹, indicating good thermal stability of the mixture, which is also consistent with this statement low thermal conductivity value of 9.38 W/mK compared to 44.8 W/mK for the unfired sample. Finally, it is concluded that the 20:80 mixture of Sabon-Gari: Bandawa clays meets the necessary conditions for use in the production of refractory materials for lining furnaces in the metalworking industry.

DOI: <https://dx.doi.org/10.4314/jasem.v29i3.4>

License: [CC-BY-4.0](https://creativecommons.org/licenses/by/4.0/)

Open Access Policy: All articles published by **JASEM** are open-access and free for anyone to download, copy, redistribute, repost, translate and read.

Copyright Policy: © 2025. Authors retain the copyright and grant **JASEM** the right of first publication. Any part of the article may be reused without permission, provided that the original article is cited.

Cite this Article as: IDU, H. K; SILAS, E (2025) Characterization of Potential Refractory Utilization of Blended Sabon-Gari and Bandawa Clays Collected from Deposits in Jalingo and Karim-Lamido Local Government Areas, Taraba State, Nigeria. *J. Appl. Sci. Environ. Manage.* 29 (3) 713-723

Dates: Received: 12 February 2025; Revised: 28 February 2025; Accepted: 09 March 2025; Published: 31 March 2025

Keywords: Clays; refractories; vibrations; ceramics; transmittance

Technological development in Nigeria has raised awareness and raised the standard of living of both urban and rural residents, resulting in increased use of modern industrial equipment. The availability of abundant natural resources in Nigeria therefore requires a shift towards intensive scientific and technological research to improve the utilization of locally available resources and to produce or improve new technologies to meet the needs of our local industries, particularly the industrial Iron and steel industry. If Nigeria is to sustain greater industrial

growth, the iron and steel industries must be maintained, and new ones must be established. These industries use kilns, and these kilns are lined with refractory bricks made from clay. Unfortunately, these fireproof materials are currently imported (Irabor and Okunkpolor, 2020; Adekeye *et al.*, 2019; Adamu *et al.*, 2018). Refractory materials are inorganic materials that can withstand high temperatures (usually above 1500 °C) under the physical and chemical action of molten metal, slag and gases in the furnace. Fire resistance, on the other

*Corresponding author, Email address: iduhyacinthkevin@gmail.com

*ORCID: <https://orcid.org/0000-0002-2555-8946>

*Tel: +2347087005115

hand, refers to the ability of refractory materials to resist melting at high temperatures; prevent heat flow across its cross-sectional boundary layer as much as possible; Maintain volume stability at high temperatures (linear expansion, areal expansion and cubic expansion must be acceptable); withstand unstable thermal and physical shocks; resist abrasion and corrosion; have higher heat resistance; and be resistant to hot liquids (gases and liquids) (Hossain and Roy, 2019; Hernández *et al.*, 2019). In addition, refractory materials must be dense and porous; therefore, insulating refractory clays are refractory materials with high porosity, low thermal conductivity and high thermal insulating properties (Elavarasan *et al.*, 2019). Refractory products are required for various processes in the chemical, ceramics, petrochemical, oil, foundry and iron and steel industries. Unfortunately, due to the ailing state of the Nigerian iron and steel sector, there is no refractory industry in Nigeria, although there are abundant deposits of clay and other raw materials needed for the production of refractory products (Nwannenna *et al.*, 2015; Nwuzor *et al.*, 2018). Regardless, there is a need for refractories in Nigeria. The potential of a developing industrial nation is enormous. For example, small-scale industries in Nnewi, a young rural industrial town in southeastern Nigeria, have been producing spare parts for decades. The spare parts are manufactured in high-temperature furnaces (foundry melting furnaces and heat treatment furnaces) that require refractory materials as linings. Since these refractory linings are largely sourced from abroad, the processing cost of these spare parts is generally high, which has a negative impact on the country's production economy (Ibrahim *et al.*, 2018; Ibrahim *et al.*, 2018; Mokwa *et al.*, 2019). Numerous studies have highlighted the interest in producing clay mixtures that can be used to produce refractory coatings for furnaces, coke ovens and other warming vessels (Salah *et al.*, 2017; Iyasara *et al.*, 2016; Calderón *et al.*, 2023). Many clay deposits in Nigeria have been described in detail, but many more have not. These include the large deposits in Taraba State, Nigeria, which, if carefully studied, could be used as raw materials for the production of refractory materials. Hence, the objective of this paper was to evaluate the Characterization of Potential Refractory Utilization of Blended Sabon-Gari and Bandawa Clays collected from Deposits in the Jalingo and Karim-Lamido Local Government Areas, Taraba State, Nigeria.

MATERIALS AND METHODS

Sampling of the clays: Twenty kilograms (20 kg) each of naturally bound moulding clay from Sabon-Gari and Bandawa were recovered from the deposit

located on the outskirts of Jalingo and Karim-Lamido Local Government Areas of Taraba State, Nigeria. The clay deposits were dug to a depth of 1.5 meters into the earth at four different locations using an iron excavator, and samples were collected at the same locations mentioned above and then transported to the test site. The clays were allowed to dry naturally in the sun for four (4) days. Since the clays are naturally bound, no additional additive was added before sample preparation. The clay samples were each processed into a slurry to remove organic matter and sand particles. The slurries were dewatered, and the resulting mass was air-dried. The hard mass was then crushed and sieved with BS72. The two clay samples were then mixed according to the following ratios: 100:0, 80:20, 60:40, 40:60, 20:80 and 0:100 in the order Sabon-Gari: Bandawa. Test samples were made from the mixtures and fired at 900 °C, 1000 °C, 1100 °C and 1200 °C. The experiments were carried out in the laboratory of the Faculty of Engineering, Ahmadu Bello University Zaria, Kaduna State, Nigeria.

Physicochemical properties determination: The characterization of the physical and chemical properties of clay samples was carried out on the blends as follows: Bulk density, apparent density, porosity, water absorption, cold crushing strength, dry compressive strength, refractoriness, thermal conductivity, and the morphological and elemental composition of the clay samples.

Scanning Electron Microscope (SEM): Morphology and microanalysis of the clays and the 20:80 blend were determined using an ultra-high resolution field emission scanning electron microscope (UHR-FEGSEM) equipped with energy dispersive spectroscopy (EDS). The electrons interact with atoms in the sample, producing various signals that contain information about the sample's surface topography and composition. Particle images were obtained with a secondary electron detector.

X-ray diffraction (XRD): Chemically, clays are defined by crystal structure and chemical composition. The X-ray diffraction (XRD) patterns were achieved using a PANalytical X'Pert Pro powder diffractometer with X'Celerator detector and variable divergence and receiving slits with Fe filtered $C_{\theta} - K_{\alpha}$ radiation. The phases obtained were identified using X'PertHighscore plus software. At various angles, the intensity diffracted was measured and recorded instantly on a chart, and the suited (θ) and (d) values were generated and received.

Thermal conductivity: The thermal conductivity of the clay sample was done using a thermal conductivity test machine of model HACH Sension5 from Agilent Technologies. Two different tests were carried out using the machine on the clay sample, i.e. before firing and after firing to determine the level of thermal conduction of the refractory clay. The portion of moulded brick was pinched and inserted it in a bicker of water which was read by the machine, the same process was repeated after firing.

Fourier Transform Infrared Spectroscopy (FTIR): Vibrational spectra for all samples were obtained using an Agilent Technologies Carry 630 FTIR spectrometer equipped with an infrared source, a potassium bromide beam splitter, and a highly sensitive DigiTect™ detector system. Detectors with a diameter of 1.3 mm, a width of 210 mm and a depth of 102 mm, consisting of approximately 0.6 mg of sample gently dispersed in 200 mg of KBr, were gently heated to 40 °C to control the amount of the absorbed water and in the MIR areas (4000 – 400 cm⁻¹) and with a resolution of 2 cm⁻¹ 128 consecutive scans.

RESULTS AND DISCUSSION

Physical Properties: The results of the various physical properties are shown in Figures 1 - 8.

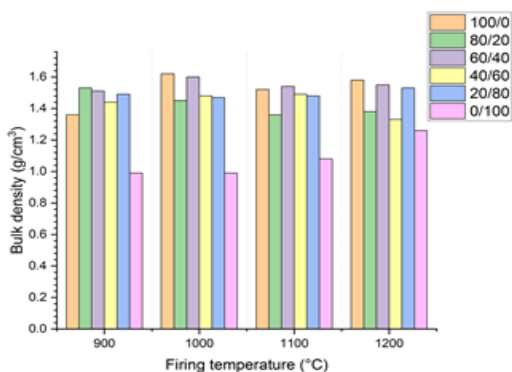


Fig. 1: Bulk density against firing temperature for the various clay blends.

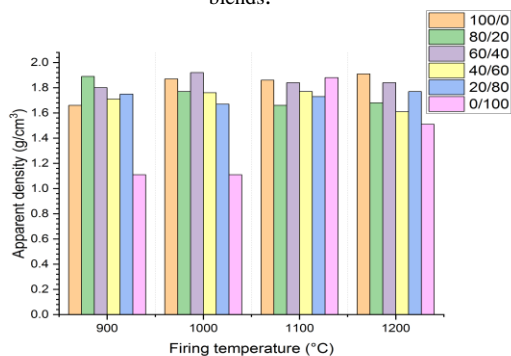


Fig.2: Apparent density against firing temperature for the various clay blends.

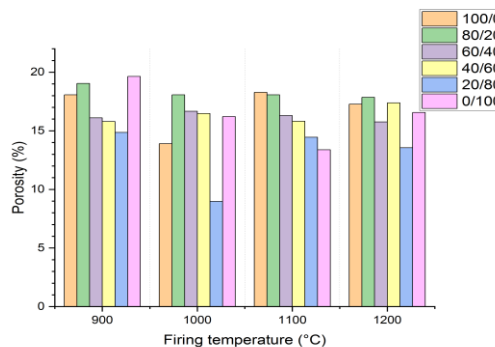


Fig. 3: Apparent porosity against firing temperature for the various clay blends.

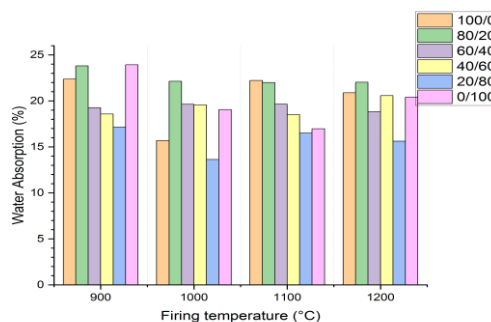


Fig. 4: Water absorption coefficient against temperature for the various clay blends.

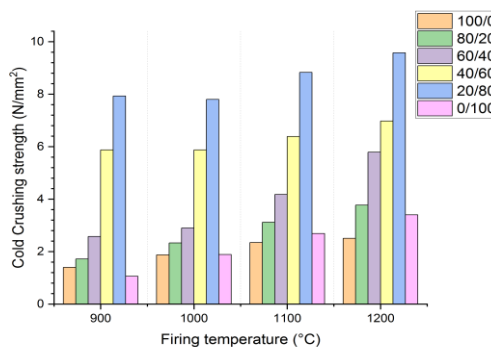


Fig. 5: Cold crushing strength (CCS) against firing temperature for the various clay blends.

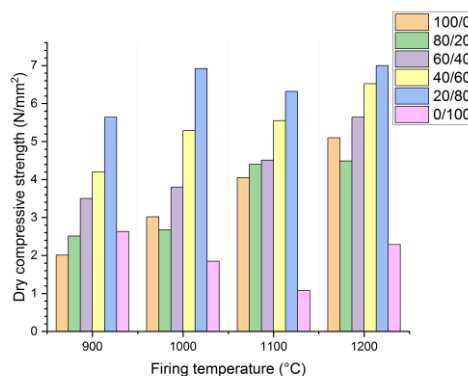


Fig.6: Dry compressive strength (DCS) (modulus of rupture) against firing temperature for the various clay blends.

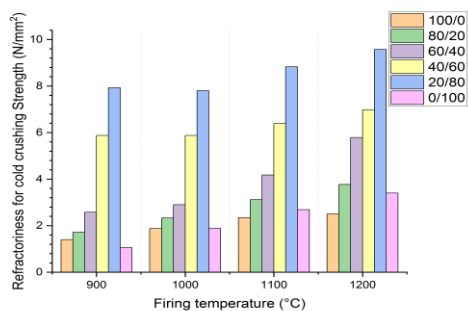


Fig. 7: Refractoriness at cold crushing strength against firing temperature for the various clay blends.

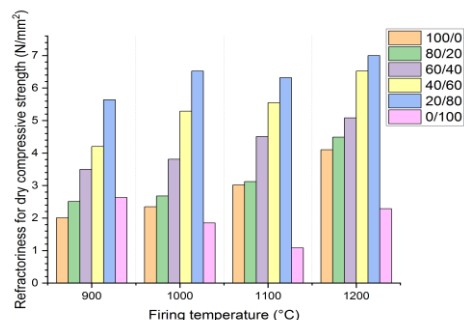


Fig. 8: Refractoriness at dry compressive strength against firing temperature for the various clay blends.

Apparent density and bulk density: These are measurements of the mass of the clay per unit volume. However, bulk density is the mass of the material per unit volume, excluding the volume occupied by the pores or voids, while apparent density is the mass of a unit volume of material, including the solid material and the pores or voids contained therein (Ituma *et al.*, 2018; Neikov *et al.*, 2019). The main difference between the two is that bulk density only takes into account the solid material with no voids, while apparent density takes into account both the solid material and pores. Again, the apparent density tends to be lower than the bulk density due to the inclusion of pore volume; the difference between the two provides information about the porosity of the material (Basu, 2013; Li and Ren, 2011; Rodriguez-Ramirez *et al.*, 2012). It is important to remember that lower apparent density values, which often indicate higher porosity, may indicate reduced resistance to thermal shock, increased water absorption, or reduced mechanical strength. Consequently, knowledge of both densities in ceramic helps in assessing the quality, robustness and applicability of the material for specific uses. For example, higher strength and lower porosity make higher bulk densities ideal for load-bearing applications (Yang and Wen, 2020; Gupta and Shaik, 2005; Zhao *et al.*, 1993). Both bulk density and bulk density typically increase with an increase in firing

temperature. The main cause of this is particle compaction and reduced porosity. According to **Figures 1 and 2**, the 20:80 mix produced the best results for these densities of all the mixes examined, indicating that all mixes in this study followed this established trend.

Apparent porosity: Apparent porosity directly affects the quality and performance of the material. Lower apparent porosity indicates a denser material with fewer voids, which typically translates into better mechanical strength, resistance to thermal shock, and improved performance in various applications (Balczar *et al.*, 2015; Machmud *et al.*, 2016). In particular, apparent porosity is a crucial factor in determining the suitability of ceramics for various applications. Understanding, measuring and controlling this parameter is critical to achieving the desired material properties, performance and functionality of ceramic products (Machmud *et al.*, 2016; Zhang *et al.*, 2022; Araujo *et al.*, 2022; Lin *et al.*, 2019). At lower firing temperatures, clays tend to have higher porosity because they are less dense and have more voids or spaces between particles. As the firing temperature increases, the particles fuse more tightly, reducing porosity and making the clay more compact. It can be seen that the clays examined follow this trend and it is clear from **Figure 3** that the 20:80 mixture had the lowest apparent porosity values across all firing temperature ranges, making it the best mixture for use in the industry.

Water absorption coefficient: This property refers to the percentage of water that the clay absorbs when immersed in water or exposed to water for a certain period. It is an essential indicator of the quality and porosity of clay. Lower absorption often indicates a denser and less porous material, which generally results in better mechanical strength, durability and resistance to environmental factors such as freeze-thaw cycles (Bomberg *et al.*, 2005; Mukhopadhyaya *et al.*, 2002). The water absorption coefficient is influenced by factors such as clay mineralogy, particle size distribution, processing and firing conditions, among others. In the construction industry, clay bricks, tiles and ceramics with controlled water absorption coefficients are used to ensure durability and weather resistance (Sicakova *et al.*, 2017; Feng and Janssen, 2018). The water absorption coefficient of clays plays a crucial role in determining their suitability for various applications and influences their durability, strength and performance. Therefore, understanding the factors affecting water absorption enables the optimization of clay materials for various industrial and artistic applications (Babin and Stramski, 2004; Chepil,

1950). Lower firing temperatures often result in higher water absorption coefficients due to increased porosity, while higher firing temperatures reduce water absorption as the clay becomes denser and less porous. Although all mixtures exhibited this behaviour, it can be shown from **Figure 4** that the 20:80 mixture has the lowest water absorption coefficient at all firing temperatures, making it the preferred mixture for use.

Cold crushing strength (CCS) and dry compressive strength (DCS): Cold compressive strength is the ability of a material to withstand a compressive load without breaking or crumbling. It is often used to assess the strength of refractory materials such as ceramics or bricks under compression (Carter and Norton, 2007; Kingery *et al.*, 1976; Wachtman *et al.*, 2009). This is different from the modulus of rupture, which measures the ability of a material to withstand bending or fracture under a bending load and is most often applied to metals, wood or concrete to determine their resistance to bending or bending stress (Rahaman, 2003; Ring, 2015; Bundiski *et al.*, 2013). Dry compressive strength is a broader term and includes the compressive strength of various materials (including clay) when tested in the dry state. The focus is not necessarily on fireproof materials or specifically on cold temperatures. For example, the dry compressive strength of clays assesses their ability to withstand compressive loading without moisture. Still, it does not consider the severe temperature conditions associated with CCS (Zhang *et al.*, 2022; Kieback and Travitzky, 2002; Wei *et al.*, 2022; Richerson, 1992). Cold compression strength (CCS) and dry compression strength increase with firing temperature. From Figures 5 and 6, it can be seen that among all the mixtures, the 20:80 mixture of Sabon-Gari-Bandawa clays had the highest values for both strengths in this order: 9.6 Nmm⁻² for CCS and 7.2 Nmm⁻² for DCS.

Refractoriness: Refractoriness is the ability of a material to withstand high temperatures without deforming or softening. The refractoriness of ceramics is influenced by factors such as composition, crystal structure and manufacturing process. Materials with high melting points such as aluminium oxide (Al₂O₃), silicon oxide (SiO₂) and zirconium oxide (ZrO₂) have excellent refractoriness. Their strong atomic structures and high melting temperatures make them ideal for applications requiring heat resistance (Ojo *et al.*, 2014; Lomertwala *et al.*, 2019; Olalere *et al.*, 2020). Ceramic materials with a stable crystal structure tend to retain their strength and integrity at high temperatures. For example, some ceramics possess a

crystalline lattice structure that remains stable even at extreme temperatures, contributing to their refractory nature (Musa *et al.*, 2012; Musa *et al.*, 2012; Odewole, 2023). The method used to form ceramics, whether through sintering, pressing or other techniques, can affect its microstructure and therefore its ability to withstand high temperatures. However, despite their excellent fireproof properties, ceramics may have limitations under certain conditions. Factors such as thermal shock, sudden temperature changes or exposure to corrosive environments can affect their refractoriness and lead to cracking or degradation (Jock *et al.*, 2013; Ugwuoke *et al.*, 2017; Arthur and Gikunoo, 2020). Clays fired at higher temperatures tend to have higher refractoriness, making them more suitable for applications where high heat resistance is required. Looking critically at Figures 7 and 8, the 20:80 mix shows the highest refractoriness values under the tested conditions.

X-ray diffraction (XRD) and Fourier Transform Infrared Spectroscopy (FTIR) Analysis: The XRD and FTIR plots are shown in Figures 9 -13.

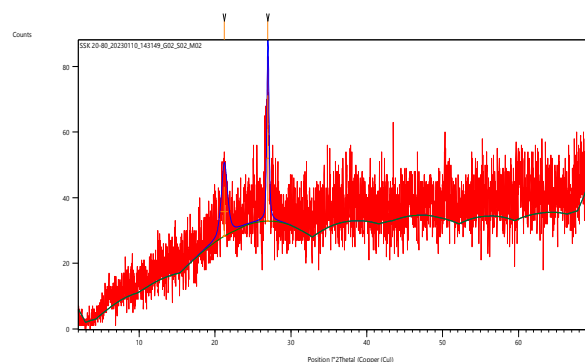


Fig. 9: X-ray diffraction pattern of Sabon-Gari clay sample.

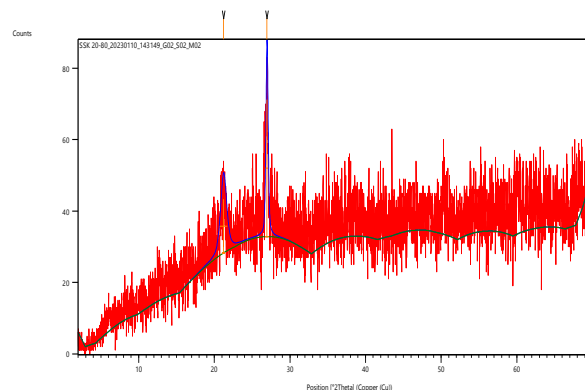


Fig. 10: X-ray diffraction pattern of Bandawa clay sample.

Mineralogy and x-ray diffraction pattern: The importance of XRD patterns in material characterization cannot be overemphasized as they provide necessary information about the crystal

structure of a material. Researchers have had to rely on it to determine a material's crystal structure, crystal orientation, lattice parameters, phase composition, and even grain size (Bunaci et al., 2015; Otwinowski and Minor, 1997; Borek et al., 2010; Ali et al., 2022; Heraldry et al., 2018). The XRD patterns of the individual samples of Sabon-Gari and Bandawa clays and the 20:80 mixture showed normal trends with prominent peaks observed at certain 2θ angles. Figure 9 shows that the Sabon-Gari clay peaked at two points, with corresponding 2θ values of 21° and 27°. In Figures 10, Bandawa clay showed peak points at 2θ angles of 21.5° and 27°. The 20:80 mixture, as shown in Figures 11, had peaks at 7 different points corresponding to 2θ angles of 21°, 24°, 26.5°, 27.5°, 30.5°, 36.5°, and 50°. When compared with existing databases, it was confirmed that these peaks correspond to (approximately) some compounds such as silicon dioxide (20.9, 26.7 and 50.7), aluminum oxide (25.7 and 35.1), iron (II) oxide (35.8) and dolomite (36.1). Mineralogical analysis of the uncovered peaks shows the significant presence of kaolinite, illite, monmorillonite, orthoclase, muscovite, albite and quartz, especially in the 20:80 mixture (Gunasekar and Krishna, 2015; Heryanto et al., 2019; Ameh, 2019; Omori et al., 2023).

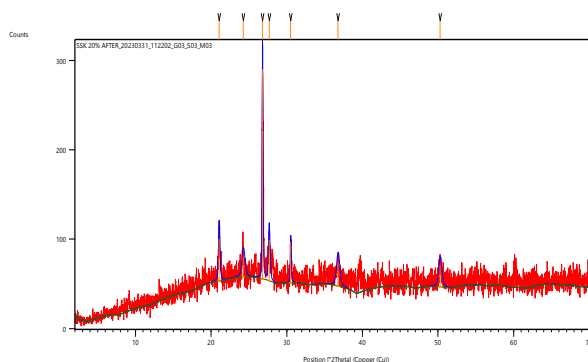


Fig. 11: X-ray diffraction pattern of blended Sabon-Gari and Bandawa clays at a ratio of 20:80 composition.

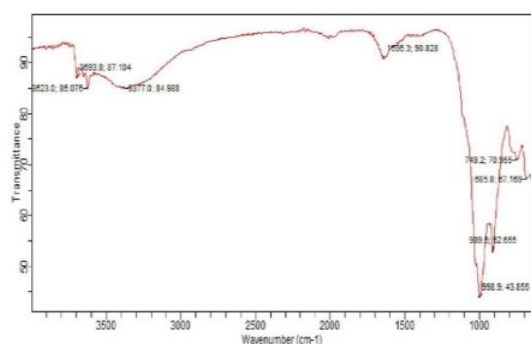


Fig. 12: (FTIR) result of the unfired 20:80 blend of Sabon-Gari and Bandawa clays sample.

Fourier Transform Infrared Spectroscopy (FTIR) Analysis: The basic concept of FTIR is that an infrared radiation (IR) spectrum represents the fingerprint of a sample, with absorption peaks that correspond to the vibrational frequencies between the bonds of the atoms that make up the material. Because each material has a unique composition and, accordingly, a different arrangement of atoms, no two compounds produce exactly the same IR spectrum.

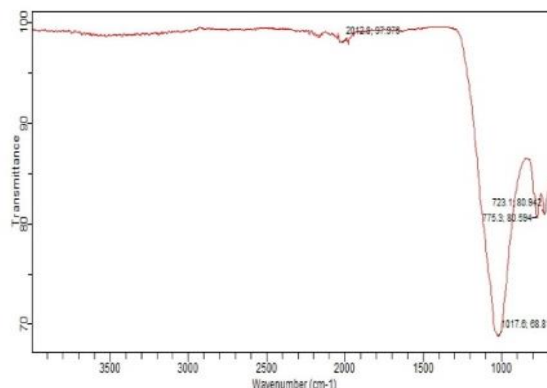


Fig. 13: FTIR of fired 20:80 blend of Sabon-Gari and Bandawa clays sample.

Therefore, IR spectroscopy can generally lead to positive identification (qualitative analysis) of any type of material. Furthermore, the size of a peak in the spectrum is a direct indication of the amount (quantitative analysis) of the particular material present in the sample (Perkins, 1986; Dutta, 2017). In the present study, both the unfired and fired samples of the 20:80 mixture were subjected to FTIR examination and the following peaks and intensities were observed in the unfired sample: 3693.8, 87.105; 3623.0, 85.075; 3377.0, 84.988; 1656.3, 90.828; 749.2, 70.955; 685.8, 67.189; 909.5, 52.655; and 998.9, 43.855, while for the fired sample we have: 2012.8, 97.978; 723.1, 80.942; 775.3, 80.594; and 1017.6, 68.817. Based on existing FTIR spectrum data, the corresponding functional groups within the unfired and fired 20:80 clay mixture at each vibration point are presented in Tables 1 and 2 (Jozanikohan and Abarghooei, 2023; Bukalo et al., 2017; Ritz et al., 2011; Ritz et al., 2012). A cursory look at the tables shows that most of the peaks/intensities observed in the unfired sample are related to the inherent water molecules in the clay that evaporated upon heating. This is consistent with established scientific concepts. Therefore, it is not surprising that only the peaks/intensities associated with the oxides and silicates were seen in the fired sample. Also, the almost constant peak/intensity level from wave number 1300 cm⁻¹ to 4000 cm⁻¹ observed in Figures

13 indicates the thermal stability of the fired sample, especially when considered together with the value of thermal conductivity coefficient in Table 3 (Leng, 2008; Plevova et al., 2011; Khang et al., 2016).

Table 1: Peak/Intensity and corresponding functional groups in the unfired 20:80 blend.

| Peak/Intensity | Functional group |
|-----------------|---|
| 3693.8 ; 87.105 | Represent the stretching vibration of the hydroxyl (OH) group, common in clays due to water absorption or structural OH groups. |
| 3623.0 ; 85.075 | Associated with the hydroxyl (OH) stretching vibration, often found in clays. |
| 3377.0 ; 84.988 | Indicating the stretching vibration of hydroxyl (OH) groups, which are prevalent in clays. |
| 1656.3 ; 90.828 | Correspond to the bending vibration of water (H ₂ O) molecules, also present due to water absorption in clay minerals. |
| 998.9 ; 43.855 | Correspond to Si-O stretching vibrations commonly seen in silicate materials, including clay minerals. |
| 909.5 ; 52.655 | Correspond to Si-O stretching vibrations commonly seen in silicate materials, including clay minerals. |
| 749.2 ; 70.955 | Attributed to the Si-O bending vibration, typical in silicate minerals found in clay. |
| 685.8 ; 67.189 | Potentially represents the Si-O-Si bending vibration, characteristic of silicate minerals in clay. |

Table 2: Peak/Intensity and corresponding functional groups in the fired 20:80 blend.

| Peak/Intensity | Functional group |
|-----------------|---|
| 2012.8 ; 97.978 | Indicate the presence of CO ₂ or carbonate species, possibly from the decomposition of carbonates during firing. |
| 1017.6 ; 68.817 | Correspond to the Si-O stretching vibration commonly seen in silicate materials. |
| 775.3 ; 80.594 | Correspond to the Si-O stretching vibration also characteristic of silicate minerals in clay. |
| 723.1 ; 80.942 | Correspond to the Si-O-Si bending vibration typical in silicate minerals found in clay. |

Scanning electron microscopy analysis: The surface morphology of the Sabon-Gari and Bandawa clays was determined using SEM. Figures 14 -15 revealed distinct differences between the unfired and fired samples. The unfired sample exhibited a rough surface with visible gaps and loosely packed particles, indicative of high porosity in Figures 14.

particle bonding and reduces pore size. These changes are consistent with a decrease in apparent porosity and water absorption, alongside an increase in bulk density. The SEM images provide direct evidence of the relationship between the microstructure and the physical properties of the Sabon-Gari and Bandawa clays studied (Aramide and Oke, 2014).

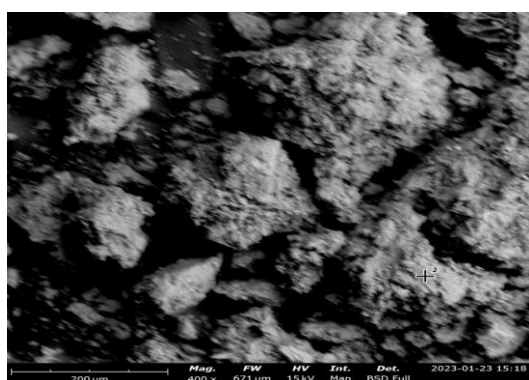


Fig.14: SEM micrograph of unfired 20:80 blend of Sabon-Gari and Bandawa clays sample.

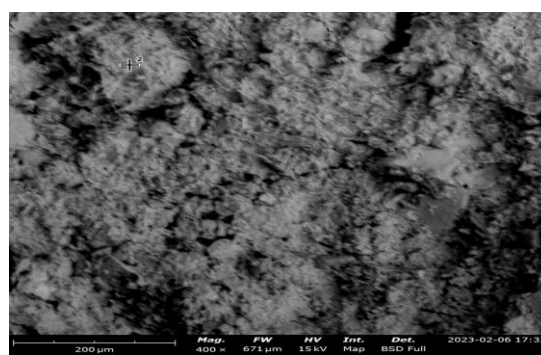


Fig.15: SEM micrograph of fired 20:80 blend of Sabon-Gari and Bandawa clays sample.

This microstructure correlates with the observed physical properties, including higher apparent porosity and water absorption coefficient, as well as lower bulk density. In contrast to Figure 15, the fired sample displayed a denser, smoother microstructure, resulting from the sintering process that promotes

Thermal conductivity analysis: From the results in Table 3, it can be observed that the thermal conductivity values of the raw and fired clay samples reflect the significant changes in their microstructural properties. The raw sample with a thermal conductivity of 44.8 W/mK allows for more efficient

heat transfer. This is due to the higher porosity and looser particle structure, which facilitates heat transport through the material (Aramide and Oke, 2014; Jastrzebska and Szczerba, 2024).

In contrast, the fired sample with a thermal conductivity of 9.38 W/mK shows a significant decrease. This reduction is due to the compression process during firing. As the material sinters, the pores shrink and the network of solid particles becomes less connected, restricting the paths for heat flow. In addition, the residual air trapped in the pores acts as an insulating barrier and reduces the material's ability to conduct heat. Although the firing process improves the strength and density of the material, it also reduces its thermal conductivity, making the fired sample more effective as a heat insulator compared to the raw sample

Table 3: Thermal Conductivity of the 20:80 blend of Sabon-Gari and Bandawa clays sample

| No | Sample: 20:80 Sabon-Gari/Bandawa blend | Conductivity (W/mK) |
|----|--|---------------------|
| 1 | Raw Sample | 44.8 |
| 2 | Fired Sample | 9.38 |

Conclusion: The results show that a 20:80 mixture of Sabon-Gari and Bandawa clays in this ratio had the best technological properties for refractory applications. This new finding suggests that efforts should be made to explore, exploit and utilize these clays for the production of refractory bricks in Nigeria to stem the tide of importation of refractory bricks into the country, thereby increasing the use of local materials to conserve the country's already scarce foreign exchange income.

Disclosure statement: *Conflict of Interest:* The authors declare that there are no conflicts of interest.

Compliance with Ethical Standards: This article does not contain any studies involving human or animal subjects.

REFERENCES

- Adamu, HA; Ibrahim, ME; Isah, IK; Jimoh, SO (2018). Investigating the refractory property of Jalingo clay deposit. *Intern. J. Sci. Eng. Res.* 9: 253-258.
- Adekeye, D; Olugbenga, P; Ibigbami, O; Asaolu, S; Olatoye, R (2019). Physicochemical characterization and mineralogical evaluation of Ire-Ekiti clay deposit in Southwestern Nigeria. *Intern. J. Eng. Appl. Sci. Technol.* 4(1): 94-99.
- Ali, A; Chian, YW; Santos, RM (2022). X-ray diffraction techniques for mineral characterization: A review for engineers of the fundamental applications and research directions, *Miner.* 12(4): 205-230.
- Ameh, ES (2019). A review of basic crystallography and x-ray diffraction applications. *Interna. J. Adv. Manu. Technol.* 105: 3289-3302.
- Aramide, FO; Oke, SR. (2014). Production and characterization of clay bonded carbon refractory from carbonized palm kernel shell, *Bull. Eng. T.* 134-140.
- Araujo, ED; Silva, KR; Grilo, JPF (2022). Dielectric properties of steatite ceramics produced from talc and kaolin wastes. *Mat. Res.* 25: e20210428.
- Arthur, EK; Gikunoo, E (2020). Property analysis of thermal insulating materials made from Ghanaian anthill clay deposits, *Cog. Eng.* 7:1-19.
- Babin, M; Stramski, D (2004). Variations in the mass-specific absorption coefficient of mineral particles suspended in water. *Limnol. Oceano.* 49(4): 756-767.
- Balczar, I; Korim, T; Dobradi, A (2015). Correlation of strength of apparent porosity of geopolymers: Understanding through variations of setting time. *Const. Buil. Mater.* 93(2): 983-988.
- Basu, S (2013). *Introduction to metal-ceramic technology.* CRC Press, Florida, USA.
- Bomberg, M; Pareza, P; Plagge, R. (2005) Analysis of selected water absorption coefficient measurements, *J. Therm. Envelo. Buil. Sci.* 28(10): 227-243.
- Borek, D; Cymborowski, M; Machius, M; Minor, W; Otwinowski, Z (2010). Diffraction data analysis in the presence of radiation damage. *Acta. Cryst.* D66, 426-436.
- Bukalo, NN; Ekosse, GE; Odiyo, JO; Ogola, JS (2017). Fourier transform infrared spectroscopy of clay size fraction of cretaceous-tertiary kaolins in the Douala sub-basin, Cameroon. *Op. Geosci.* 9: 407-418.
- Bunaci, AA; Udristioiu, EG; Aboul-Enein, HY (2015). X-ray diffraction: Instrumentation and applications, *Cri. Rev. Analyt. Chem.* 45(4): 289-299.

- Bundiski, KG; Bundiski, MK (2013) *Engineering Materials: Properties and selection*. Pearson Prentice Hall.
- Calderón, S; Sandoval, C; Araya-Letelier, G; Aguilar, V (2023). A detailed experimental mechanical characterization of multi-perforated clay brick masonry. *J. B. Eng.* 63(4): 105505.
- Carter, CB; Norton, MG (2007). *Ceramic Materials: Science and engineering*. Springer.
- Chepil, WS (1950). Methods of estimating the apparent density of discrete soil grains and aggregates. *Soil Sci.* 70: 351-362.
- Dutta, A (2017). Fourier transform infrared spectroscopy. In: Thomas, S., Thomas, R., Zachariah, A. K., & Mishra, R. K. (Eds.) *Spectroscopic Methods of nanomaterials characterization*, Amsterdam: Elsevier, 74-95.
- Elavarasan, S; Priya, AK; Kumar, V. K. (2019). Manufacturing fired clay brick using fly ash and M-sand. *Mater. Today: Proc.* 37: 872-876.
- Feng, C; Janssen, H (2018). Hygric properties of porous building materials (III): Impact factors and data processing methods of capillary absorption test. *Buil. Environ.* 134: 21-34.
- Gunashekar G. S., Krishna M. (2015). An overview on powder x-ray diffraction and its current applications. Research and Reviews. *J. Phy.* 4(2): 6-10.
- Gupta, RC; Shaik, AA (2005). DRI apparent density and its strength. *ISIJ Interna.* 45: 408-409.
- Herald, E; Cahyo, SAN; Indri, NA; Rahmawati, F (2018). X-ray diffraction analysis on the effect of time reaction and alkali concentration in merlinoite. *J. Phy.* 1095: 1-5.
- Hernández, AC; Sánchez-Espejo, R; Meléndez, V; González, G; López-Galindo, A; Viseras, C (2019). Characterization of Venezuelan kaolins as health care ingredients. *Appl. Clay Sci.*, 175: 30-39.
- Heryanto, H; Abdulla, B; Tahir, D; Mahdalia, M (2019). Quantitative analysis of x-ray diffraction spectra for determining structural properties and deformation energy of Al, Cu and Si. *J. Phy.* 1317: 1-11.
- Hossain, SKS; Roy, PK (2019). Development of waste derived nano-lakargiite bonded high alumina refractory castable for high-temperature applications. *Ceram. Intern.*, 45, 16202-13.
- Ibrahim, ME; Adamu, HA; Isah, IK; Jimoh, SO (2018). Investigating the refractory properties of Jalingo clay deposit. *Intern. J. Sci. Eng. Res.* 9: 241-250.
- Irabor, EEI; Okunkpolor, AK (2020). Physico-chemical and mineralogical properties of a clay mineral deposit in Geheku, Kogi State, Nigeria. *JCSN.* 45(2): 698-704.
- Ituma, CG; Etukudoh, AB; Abu, M; Obioha, CI (2018). Utilization of Nkpuma-Akpatakpa clay in ceramics: Characterization and microstructural studies. *J. Appl. Sci.* 22(1): 47-56.
- Iyasara, A.C; Stan, EC; Geoffrey, O; Joseph, M; Patrick, NN; Benjamin, N (2016). Influence of grog size on the performance of NSU clay-based dense refractory bricks. *Am. J. Mater. Sci. Eng.* 4: 7-12.
- Jastrzebska, I; Szczerba, J (2024). Design, manufacturing and properties of refractory Materials. *Mater.* 17: 1673.
- Jock, A; Ayeni, F; Ahmed, A; Ilayman, U (2013). Evaluation of the refractory properties of Nigerian Ozanagogo clay deposit, *J. Min. Mater.Ch. Eng.* 1: 321-325.
- Jozanikohan, G; Abarghoeei, MN (2023). The Fourier transform infrared spectroscopy (FTIR) analysis for the clay mineralogy studies in a elastic reservoir, *J. Petro. Explor. Prod. Technol.* 12 (4): 2093-2106.
- Khang, VC; Korovkin, MV; Ananyeva, LG (2016). Identification of clay minerals in reservoir rocks by FTIR spectroscopy, *IOP Conf. Series: Earth Environ. Sci.* 43: 012004.
- Kieback, N; Travitzky, N (2002). *Reinforcements and additions in ceramic processing*. Wiley-VCH, Germany.
- Kingery, WD; Bowen, HK; Uklmann, DR (1976). *Introduction to Ceramics*. Wiley.
- Leng, Y (2008). *Materials characterization: Introduction to microscopic and spectroscopic method*, John Wiley & Sons.

- Li, Y; Ren, S (2011). *Building decorative materials*. Woodhead Publishing.
- Lin, H; Singh, M; Ohji, MT (2019). *Processing of Ceramics: Microstructure evolution*. John Wiley & Sons.
- Lomertwala, H; Njoroge, P; Opujo, SA; Ptoton, B (2019). Characterization of clays from selected sites for refractory applications. *Intern. J. Sci. Res. Pub.* 9(3): 600-603.
- Machmud, MN; Jalil, Z; Afifuddin, M (2016). Apparent porosity and compressive strength of heat-treated clay/iron sand/rice husk ash composites over a range of sintering temperatures. *Makara J. Technol.*, 20(3), 103-108.
- Mokwa, JB; Lawal, SA; Abolarin, MS; Bala, KC (2019). Characterization and evaluation of selected kaolin clay deposits in Nigeria for furnace lining application. *Nijotech.* 38(4): 936-946.
- Mukhopadhyaya, P; Kumaran, K; Normandain, N; Goudreau, P (2002). Effect of surface temperature on water absorption coefficient of building materials, *J. Therm. Envelo. Buil. Sci.*, 26(2): 179-195.
- Musa, U; Aliyu, MA; Mohammed, IA; Mohammed, AD; Sadiq, MM; Isah, AG (2012). A comparative study of the refractory properties of selected clays in Niger State, Nigeria. *Adv. Biotechnol. Chem. Proc.* 2(1): 1-5.
- Musa, U; Aliyu, MA; Mohammed, IA; Mohammed, AD; Sadiq, MM; Isah, AG (2012). A comparative study of the refractory properties of selected clays in North Central, Nigeria, *Acad. Res. Intern.* 3: 393-398.
- Neikov, O; Naboychenko, S; Yefimov, NA (2019). *Handbook of non-ferrous metal powders: Technologies and applications*. Elsevier, Amsterdam, Netherlands.
- Nwannenna, OC; Apeh, FI; Ogunro, AS; Fabiyi, MO (2015). Characterization of Ibamajo, Moye and Nkwo-Alaike fireclays for use as refractory materials in the foundry industry. *Chem. Proc. Eng. Res.* 35(4): 65-76.
- Nwuzor, IC; Chukwunke, JL; Nwanonyi, SC; Obasi, HC; Ihekwe, GO (2018). Modification and physiochemical characterization of kaolin clay for adsorption of pollutants from industrial paint effluent. *Eur. J. Adv. Eng. Technol.* 5(1): 609-620.
- Odewole, OA (2023). Investigation on the physicochemical properties of Nru clay deposit and its industrial application, *IOP Conf. Ser.: Earth Environ. Sci.* 1178: 012025.
- Ojo, J; EKutebe, BJ; Oshuoha, IC (2014). Effect of blending on the refractory properties of some selected local clays in South Western Nigeria. *J. Res. Mech. Eng.* 2(1): 1-5.
- Olalere, AA; Yaru, SS; Olurotimi, AD (2020). Evaluation of the chemical and thermophysical properties of locally aggregated kaolin-based refractory materials. *J. Mech. Eng. Sci.* 13(5): 4743-4755.
- Omori, NE; Bobitan, AD; Vamvakeros, A; Beale, M; Jacques, SDM (2023) Recent developments in x-ray diffraction/scattering computed tomography, *Phil. Trans. R. Soc. A*, 381, 2022035D.
- Otwinowski, Z; Minor, W (1997). Processing of x-ray diffraction data. *Meth. Enzymol.* 276c: 307-326.
- Perkins, WD (1986). Fourier transform-infrared spectroscopy, part 1, instrumentation. Topics in chemical instrumentation, in: Settle, F. A. (Ed.). *J. Chem. Educ.*, 63, A5-A10.
- Plevova, E; Vaculikova, L; Kozusnikova, A; Danek; T; Pleva, M; Ritz, M; Martynkova, GS (2011). Thermal study of sandstones from different Czech localities, *J. Therm Anal Calorim.* 103(8), 835-843. Rahaman M. N., (2003) *Ceramic Processing and Sintering*, 2ed. Marcel Dekker, New York.
- Richerson, DW (1992). *Introduction to ceramics*. John Wiley & Son.
- Ring, TA (2015). *Fundamentals of ceramic powder processing and synthesis*, Wiley.
- Ritz, M; Vaculikova, L; Plevova, E; Matysek, D; Malis, J (2012). Determination of chlorite, muscovite, albite and quartz in claystones and clay shales by infrared spectroscopy and partial least-squares regression, *Acta. Geodyn. Geomater.* 9:511-520.

- Ritz, M; Vaculikova; L; Plevova; E (2011). Application of infrared spectroscopy and chemometric methods to identification of selected minerals, *Acta Geodyn. Geomater*, 8, 47-58.
- Rodriguez-Ramirez, J; Mendez-Lagunas, A; Lopez-Ortiz, S; Torres, S. (2012). True density and apparent density during the drying process for vegetables and fruits: A review. *J. Food Sci.* 77(4): R146-R154.
- Salah, M; Ali, B; Ezzedine, S; Fouad, Z (2017). Characterization, firing behaviour and ceramic application of clays from the Gabes region in South Tunisia. *Appl. Clay Sci.* 135: 215-225.
- Sicakova, A; Draganovska, M; Kovac, M (2017) Water absorption coefficient as a performance characteristic of building mixes containing fine particles of selected recycled materials. *Proc. Eng.* 180(20): 1256-1265.
- Ugwuoke, JC; Amalu, NI (2017). Characterization of Obe clay deposit for refractory production, *Am. J. Eng. Res.* 6(6): 74-77.
- Wachtman, JB; Cannon, WR; Matthewson, MJ (2009) *Mechanical Properties of Ceramics*. John Wiley & Sons Ltd.
- Wang, B; Tu, R; Wei, Y; Cai, H (2023). Self-healing of SiC-Al₂O₃-B₄C ceramic composites at low temperatures. *Mater.* 15: 652.
- Wei, ZY; Meng, GH; Chen, L (2022). Progress in ceramic materials and structure design towards advanced thermal barrier coatings, *J. Adv. Ceram.*, 11, 985-1068.
- Yang, X.; Wen, J (2020). Study on factors influencing the performance of reactive powder concrete. *IOP Conf. Ser.: Earth Environ. Sci.*, 510(2) 052075.
- Zhang, X; Zhang, K; Zhang, B; Li, Y; He, R (2022). Mechanical properties of additively-manufactured cellular ceramic structures: A comprehensive study. *J. Adv. Ceram.* 11: 1918-1931.
- Zhang, Y; Yu, L; Wang, J; Mao, H; Cui, K (2022). Microstructure and mechanical properties of high-strength porous ceramics with high sewage sludge content. *J. Clean. Prod.* 380(7): 135084.
- Zhao, R; Cavalleri, RP; Hyde, GM; Pitts, MJ (1993). Apparent density of air-water mixtures. *ASAE*. 36(1): 103-111.